$$\langle \tau_N \rangle = \int_0^\infty [1 - [1 - S(t)]^N] \, dt \quad (6)$$

To calculate $S(t)$, we note that in spherical coordinates, the probability density for a Brownian particle to go from $\mathbf{r}_0$ to $\mathbf{r}$ at time t is

$$p(\mathbf{r},t|\mathbf{r}_0,0) = 4\pi\left(\frac{3}{4\pi D_s t}\right)^{3/2} \exp\left[-\frac{3(\mathbf{r}-\mathbf{r}_0)^2}{4D_s t}\right] \quad (7)$$

where D_s is the diffusion constant for a single chain. Hence, the probability that the Brownian particle is within the sphere at time t is

$$S(t) = 4\pi\left(\frac{3}{4\pi D_s t}\right)^{3/2} \int \cdots \int \exp\left[-\frac{3(\mathbf{r}-\mathbf{r}_0)^2}{4D_s t}\right] d\mathbf{r}\, d\mathbf{r}_0 \quad (8)$$

where $\mathbf{r}_0$ and $\mathbf{r}$ take all values inside the sphere. When t is sufficiently large that $D_s t \gg R^2$, the exponential tends to the limit 1 and the integral tends toward V^2, where V is the volume of the sphere. Hence, we find

$$S(t) \sim (2\pi)^{1/2}(R^2/D_s t)^{3/2} \quad (9)$$

When the number of Brownian particles, N, is large, we may rewrite eq 6 as

$$\langle \tau_N \rangle \sim \int_0^\infty (1 - e^{-NS(t)}) \, dt \quad (10)$$

From this form it is evident that the integrand is very close to 1 as long as $NS(t) \gg 1$ and only goes to zero when $S(t) \sim 1/N$, which is in the region in which the asymptotic representation in eq 8 is valid. Hence, we may write

$$\langle \tau_N \rangle \sim \int_0^\infty (1 - e^{-N(T_0/t)^{3/2}}) \, dt = T_0 N^{2/3} \int_0^\infty (1 - e^{-x^{-3/2}}) \, dx \quad (11)$$

in which

$$T_0 = AR^2/D_s \quad (12)$$

where A is a dimensionless constant of no importance to the argument.

In order to translate Kesten's result into the language of the reptation problem, we note that the radius of the sphere scales as $M^{1/2}$, N also scales as $M^{1/2}$, and D_s scales as M^{-2}. Thus

$$\tau_r \sim \frac{M^{1+1/3+2}}{(\ln M)^{2/3}} = \frac{M^{10/3}}{(\ln M)^{2/3}} \quad (13)$$

The dominant factor in this last equation is $M^{10/3}$ while the logarithmic term would only be detectable when measurements are made over many orders of magnitude of the mass.

Conclusions

Within de Gennes's original reptation model of kink-generated motion, we follow Scher–Shlesinger to treat the measured polymer melt diffusion constant as a single chain quantity and the reptation time as a multichain quantity to reconcile for the first time the experimentally observed and theoretical compatible results $D \sim M^2$ and $\tau_r \sim M^{10/3}/(\ln M)^{2/3}$ in which the logarithmic term would not ordinarily be detectable.

References and Notes

(1) de Gennes, P.-G. *J. Chem. Phys.* **1971**, *55*, 572. de Gennes, P.-G. *Scaling Concepts in Polymer Physics*; Cornell University Press: Ithaca, NY, 1979.
(2) Doi, M.; Edwards, S. F. *J. Chem. Soc.* **1978**, *74*, 1780, 1802, 1818; *J. Chem. Soc., Faraday Trans. 2* **1979**, *75*, 38.
(3) Klein, J. *Macromolecules* **1978**, *11*, 852.
(4) Graessley, W. W. *Adv. Polym. Sci.* **1982**, *47*, 67.
(5) Klein, J.; Briscoe, B. *Proc. R. Soc.* London, A **1979**, *365*, 53.
(6) Leger, L.; Hervet, H.; Rondelez, F. *Phys. Rev. Lett.* **1979**, *52*, 1681.
(7) Callaghan, P.; Pinder, D. *Macromolecules* **1980** *13*, 1085; **1981**, *14*, 1334.
(8) Ferry, J. D. *Viscoelastic Properties of Polymers*; Wiley: New York, 1980; p 241 ff.
(9) Kolinski, A.; Skolnick, J.; Yaris, R. *J. Chem. Phys.* **1986**, *86*, 1567.
(10) Doi, M. *J. Polym. Sci., Polym. Phys. Ed.* **1983**, *21*, 667.
(11) Rubinstein, M., preprint.
(12) Deutsch, J. M. *Phys. Rev. Lett.* **1985**, *54*, 56.
(13) Wendel, H.; Noolandi, J. *Macromolecules* **1982**, *15*, 1313.
(14) Scher, H.; Shlesinger, M. F. *J. Chem. Phys.* **1986**, *84*, 5922.
(15) Green, M. S.; Tobolsky, A. V. *J. Chem. Phys.* **1964**, *14*, 80.
(16) Lodge, A. S. *Rheol. Acta* **1968**, *7*, 379.
(17) Bendler, J. T.; Dishon, M.; Kesten, H.; Weiss, G. H. *J. Stat. Phys.*, in press.

Downloaded via UNIV SCIENCE AND TECHNOLOGY CHINA on May 13, 2020 at 03:15:58 (UTC).
See https://pubs.acs.org/sharingguidelines for options on how to legitimately share published articles.

Communications to the Editor

Synchrotron Small-Angle X-ray Scattering of Sulfonated Polystyrene Ionomers

The field of ion-containing polymers, with its many industrial applications, has undergone explosive growth in recent years.[1] Nevertheless, a fundamental understanding of the spatial arrangement of the ionic groups in ionomers has remained elusive. Initial theoretical developments by Eisenberg,[2] MacKnight et al.,[3] Yarusso and Cooper,[4] and Fujimura et al.[5] have led to the concepts of ion pair, multiplet, and cluster formation as well as inter- and intraparticle interactions among the ion pairs, multiplets, or clusters. The models of the structure of ionomers are based mainly on results from small-angle X-ray scattering (SAXS) and electron microscopy. While transmission electron micrographs may suggest the presence of ion aggregates or domains, the details of ion distribution can best be achieved by using SAXS. Earlier SAXS profiles[4-7] of metal salts of sulfonated polystyrene (S–PS) show only one ionic peak occurring at the scattering vector $q \sim 1.7$ nm^{-1} where $q = (4\pi/\lambda) \sin(\theta/2)$ with λ and θ being the X-ray wavelength and the scattering angle, respectively. The absence of "fine" structure in the scattering profile means that the experimental data with finite q range and precision can be interpreted by using a variety of models.[3-5] Unfortunately, the details of the spatial arrangement of the ionic groups cannot be retrieved from scattering data on the ionic peak alone.

The radial distribution function (RDF) approach which is essentially model independent and is applicable to the structural determination of amorphous materials in general has been used to analyze the SAXS profile.[3,8] In the absence of reliable scattering data in the asymptotic small-

0024-9297/88/2221-0523$01.50/0 © 1988 American Chemical Society

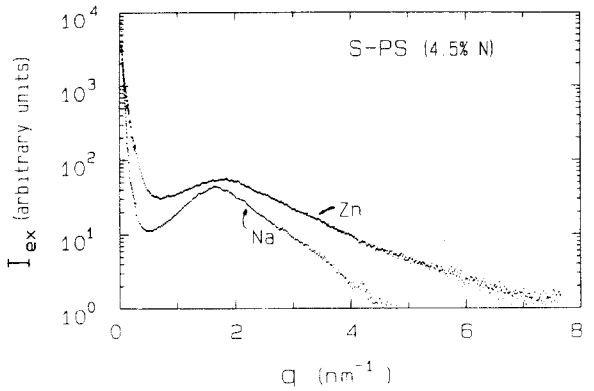

Figure 1. Semilog plot of excess scattered intensity versus q (nm^{-1}) for sodium and zinc salts of narrow (N) molecular weight distribution sulfonated polystyrene (S–PS). PS: M_w = 1.15 × 10^5 g/mol, M_w/M_n = 1.04; 4.5 mol % sulfur, 100% neutralized.

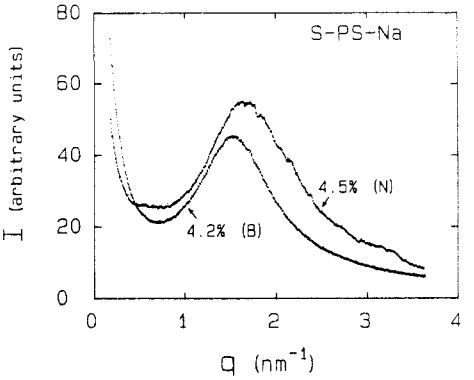

Figure 2. Plot of scattered intensity versus q (nm^{-1}) for sodium salts of narrow and broad molecular weight distribution (MWD) sulfonated polystyrene. Mol % sodium = 4.5 and 4.2 for narrow (N; M_w/M_n = 1.04) and broad (B; M_w/M_n = 2.66) MWD, respectively. PS M_w = 1.15 × 10^5 g/mol.

angle region, the RDF approach did not reveal the details of the (long range) spatial arrangement of ionic groups in the ionomer.

Synchrotron radiation with its high flux and well-defined X-ray wavelengths is an ideal tool to investigate the detailed SAXS profiles which are not accessible by standard X-ray sources. In this paper, we report that precise SAXS curves of sodium and zinc salts of sulfonated polystyrene can be measured over a very broad q range (0.03 nm^{-1} $\lesssim$ q $\lesssim$ 8 nm^{-1}). Furthermore, as we are interested in the excess scattered intensity due to ions in the ionomer, the polystyrene backbone scattering curve is subtracted from the scattering curves of the ionomers.

In the present experiment, we used well-annealed S–P-S–Na and S–PS–Zn samples with PS M_w = 1.15 × 10^5 g/mol, M_w/M_n = 1.04 or 2.66, and a sulfur content of ~4.5 mol %, 100% neutralized. A new modified Kratky block collimation system[9] has been adapted successfully at X21A2 State University of New York (SUNY) beamline, National Synchrotron Light Source, Brookhaven National Laboratory. With a slit width of ~0.5 mm, a λ = 0.154 nm, and a sample to detector distance of 250 mm, we were able to reach θ ~ 0.075 mrad corresponding to q ~ 0.03 nm^{-1} (or a Bragg spacing of ~200 nm). The scattering profiles have been corrected for absorption which was measured independently by using two ionization chambers located before and after the S–PS sample, sample thickness which was measured using a micrometer gauge, parasitic scattering, incident X-ray intensity fluctuations due to the position instability of the synchrotron radiation and the intrinsic lifetime of the storage ring, and detector nonlinearity. The excess scattered intensity (I_{ex}) denotes the corrected scattered intensity of the ionomer minus the corrected scattered intensity of the same polystyrene (without ions). The excess scattered intensity has been normalized to per second and per millimeter sample thickness and each of the 850 data points were treated individually without smoothing. Measurement time for each scattering curve was of the order of 1000 s.

Figure 1 shows a semilog plot of the net SAXS curve of S–PS–Na and S–PS–Zn over a very broad q range (0.03 nm^{-1} $\lesssim$ q $\lesssim$ 8 nm^{-1}). Measurements at very small scattering angles permit us to obtain a reliable extrapolation of the scattered intensity to zero scattering angle. Subtraction of the polystyrene backbone background (without arbitrary adjustment) reveals that we were able to measure the net SAXS curve to large values of q where the ionic intensity has decayed to near zero. We were able to cover the scattered intensity over a factor of >10^4.

Figure 2 shows a plot of scattered intensity versus q for S–PS–Na with broad (B; M_w/M_n = 2.66) and narrow (N; M_w/M_n = 1.04) molecular weight distributions (MWD) of the polystyrene backbone. In the semilog plot of Figure 1, we display the complete net scattering curve due to the ionic groups. In Figure 2, we amplify the ionic peak region to show the presence of fine structure for the S–PS–Na(N). The experiment was reproducible by using two different linear position sensitive detectors (a Braun LPSD and an EG&G photodiode array detector) on two separate S–P-S–Na samples. Furthermore, the fine structure disappears for the broad MWD S–PS–Na sample suggesting that at least for S–PS–Na (4.5 mol %, N) some features which have not been observed previously are worthy of further studies. It should be noted that the finite beam cross section of even the synchrotron beam could smear the fine structures. However, desmearing of the SAXS curve should only increase the contrast in the fine structures.

From Figures 1 and 2, we can make the following observations. (1) The ionic peak height is more than 100 times smaller than the scattered intensity extrapolated to zero scattering angle. Thus, the small angle region (q < 0.03 nm^{-1}) makes a very important contribution in the net SAXS curve and cannot be ignored. (2) Zinc and sodium salts of S–PS show similar q_{max} ~ 1.7 nm^{-1}. (3) The Zinc ionic peak is broader. (4) No fine structure and secondary peak are observed in the S–PS–Zn curve. (5) S–PS–Na(N) appears to show some fine structures which deserve further studies.

In summary, we note that precise SAXS patterns over a very broad q range can be achieved by using synchrotron radiation. Such scattering data also reveal the importance of the small-angle region and possible presence of fine structure for the narrow MWD S–PS–Na sample as well as a definitive absence of a secondary peak for the S–PS–Zn sample. A detailed analysis including the RDF approach and ion inhomogeneity in the small-angle region using the spatial correlation function concept is under way.

Acknowledgment. B.C. gratefully acknowledges support of this work by the Department of Energy (DEFGO286ER45237A001). The SUNY Beamline at the National Synchrotron Light Source is supported by a Department of Energy grant (DEFGO286ER45231A001).

References and Notes

(1) See, for examples: Eisenberg, A.; King, M. *Ion Containing Polymers*, Academic: New York, 1977. MacKnight, W. J.; Earnest, T. R., Jr. *J. Polym. Sci., Macromol. Rev.* **1981**, *16*, 41.
(2) Eisenberg, A. *Macromolecules* **1970**, *3*, 147.
(3) MacKnight, W. J.; Taggart, W. P.; Stein, R. S. *J. Polym. Sci., Polym. Symp.* **1974**, *45*, 113.

(4) Yarusso, D. J.; Cooper, S. L. *Macromolecules* **1983**, *16*, 1871; *Polymer* **1985**, *26*, 371.
(5) Fujimura, M.; Hashimoto, T.; Kawai, H. *Macromolecules* **1982**, *15*, 136; **1981**, *14*, 1309.
(6) Weiss, R. A.; Lefelar, J. A. *Polymer* **1986**, *27*, 3. Lefelar, J. A.; Weiss, R. A. *Macromolecules* **1984**, *17*, 1148.
(7) Peiffer, D. G.; Weiss, R. A.; Lundberg, R. D. *J. Polym. Sci., Polym. Phys. Ed.* **1982**, *20*, 1503.
(8) For example, see: Kao, J.; Stein, R. S.; MacKnight, W. J.; Taggart, W. P.; Cargill, G. S., III *Macromolecules* **1974**, *7*, 95.
(9) Chu, B.; Wu, D.-Q.; Wu, C. *Rev. Sci. Instrum.* **1987**, *58*, 1158.

† State University of New York at Stony Brook.
‡ University of Massachusetts.
§ State University of New York at Buffalo.
⊥ BNL.
∥ Exxon Chemical Co.

Benjamin Chu,*† Dan-Qing Wu,† W. J. MacKnight,‡ Chi Wu,† J. C. Phillips,§,⊥ A. LeGrand,⊥ C. W. Lantman,‡ and R. D. Lundberg∥

Chemistry Department, State University of New York at Stony Brook, Long Island, New York 11794-3400
Department of Polymer Science and Engineering University of Massachusetts Amherst, Massachusetts 01003
Chemistry Department, State University of New York at Buffalo, Buffalo, New York 14214
SUNY X3 Beamline, NSLS, BNL Upton, New York 11973
Paramins Division, Exxon Chemical Company Linden, New Jersey 07036

Received August 24, 1987; Revised Manuscript Received October 19, 1987

Cationic Latexes with Bound Cobalt Phthalocyaninetetrasulfonate Catalyze Autoxidation of 1-Decanethiol

The activity of heterogeneous catalysts normally increases as the catalyst particle size decreases because surface area per unit weight is inversely related to particle diameter. We report that a 60-nm diameter cationic latex with bound cobalt phthalocyaninetetrasulfonate (CoPcTs)

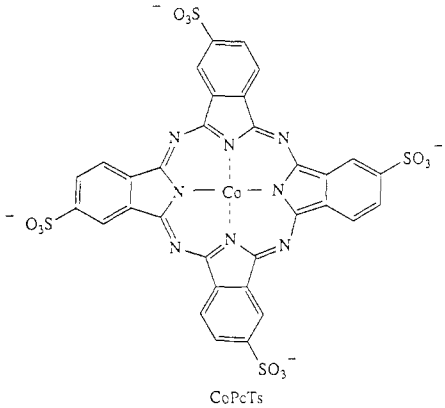

CoPcTs

is 11 times more active than soluble $CoPcTsNa_4$ for autoxidation of 1-decanethiol in water. Previously CoPcTs bound to soluble polymers has shown greater activity than $CoPcTsNa_4$ for autoxidation of 2-mercaptoethanol.[1-3] CoPcTs bound to Sephadex ion-exchange resins was less active than soluble $CoPcTsNa_4$ for autoxidations of 2-mercaptoethanol and 1-butanethiol in aqueous and nonaqueous media.[4] Autoxidation of thiols is important in industry for the removal of thiol odors (such as the "sweetening" of petroleum)[5,6] and in living organisms (such as for changes in protein structure).[7,8]

Table I
Autoxidation of 1-Decanethiol with CoPcTs Catalysts[a]

	latex 1, mg	R_4N^+, mmol	CoPcTs, mmol	1-decanethiol, mmol	pH[b]	k_{obsd},[c] mL of O_2 min^{-1}
1	0	0.0	0.0105	1.53	9.0	0.060
2	600	0.105	0.0	1.53	9.0	0.034
3	600	0.105	0.0105	1.53	9.0	0.678
4	600	0.105	0.0105	1.53	8.0	0.444
5	600	0.105	0.0105	1.53	7.0[d]	0.129
6	900	0.158	0.0158	1.53	9.0	0.724
7	79	0.014	0.0014	1.53	9.0	0.301
8	600	0.105	0.0105	0.75	9.0	0.371
9	600	0.105	0.0105	3.14	9.0	0.601
10	600	0.105	0.0105	1.53	9.0	0.20

[a] All experiments were carried out at 35.0 ± 0.1 °C and O_2 pressure of 720 mmHg (about 20 mmHg less than atmospheric pressure) with magnetic stirring of 105 mL of reaction mixture. [b] Adjusted with 4 mL of 0.0125 M $Na_2B_4O_7$ and HCl buffer. [c] Initial zero-order rate constants calculated from the plot of oxygen consumption during oxidations of decanethiol. [d] Buffered with Na_2HPO_4 and HCl.

Latexes L-1, L-2, and L-3 were prepared by emulsion copolymerization of 96.2 mol % styrene, 1.0 mol % active divinylbenzene (technical 55% active), 0.8 mol % ethylvinylbenzene, and 2.0 mol % of monomer **1**,[9] **2**, and **3** as

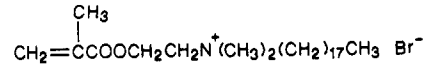

1

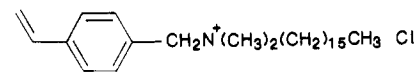

2

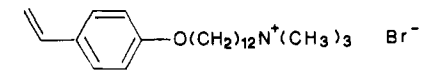

3

surfactant with azobis(isobutyronitrile) as initiator. Cross-linking with divinylbenzene ensured that the polymer remained insoluble during all subsequent experiments. Number-average particle diameters of the three latexes measured on transmission electron micrographs were 58, 64, and 58 nm (±1-nm standard deviation), respectively. The conductivity of the aqueous solution of **1** was 440 Ω^{-1} cm^{-1} before copolymerization. Ultrafiltration of the copolymer latex gave an initial filtrate with conductivity of 20–25 Ω^{-1} cm^{-1} and a final filtrate with 6 Ω^{-1} cm^{-1}. Titration of the ultrafiltered latex by the Volhard method detected 96% of the bromide ion initially charged as surfactant. IR analysis of coagulated latex showed no detectable band at 1635 cm^{-1} for the double bond of **1**. Thus the polymer colloids contained little, if any, free surfactant.

Addition of aqueous $CoPcTsNa_4$[10] to the latexes completely bound the CoPcTs to form the latex catalysts LC-1, LC-2, and LC-3. Ultrafiltration of each catalyst with a 0.1-μm cellulose acetate/nitrate membrane (Millipore) revealed no blue CoPcTs in the filtrate; 0.1 μM CoPcTs can be detected by the human eye. $CoPcTsNa_4$ is soluble in water alone or in the presence of surfactant **1**. The colloids used as catalysts contained no detectable CoPcTs in solution.

Autoxidation of 1-decanethiol at pH 9.0 in 1 atm of dioxygen with LC-1 gave 95% conversion of thiol in 30 min at 35 °C (experiment 3 in Table I), even though 1-decanethiol is immiscible with water. The catalyst suspension was held in air for 15 min before addition of thiol. The amount of thiol consumed was determined by GLC

0024-9297/88/2221-0525$01.50/0 © 1988 American Chemical Society